JACS
JOURNAL OF THE AMERICAN CHEMICAL SOCIETY

ARTICLE

pubs.acs.org/JACS

From Platonic Templates to Archimedean Solids: Successive Construction of Nanoscopic $\{V_{16}As_8\}$, $\{V_{16}As_{10}\}$, $\{V_{20}As_8\}$, and $\{V_{24}As_8\}$ Polyoxovanadate Cages

Lei Zhang and Wolfgang Schmitt*

School of Chemistry and CRANN, Trinity College, University of Dublin, Dublin 2, Ireland

Supporting Information

ABSTRACT: Supramolecular coordination cages provide unique restricted inner cavities that can be exploited for molecular recognition purposes and catalysis. Their syntheses often involve complex self-organization processes and rely on the identification of preorganized, kinetically stable building units that provide ligand-accessible coordination sites. Here we report a highly effective protocol for the successive buildup of symmetrical nanoscopic polyoxometalate (POM) cages. Our methodology takes advantage of a supramolecular templating effect and utilizes the structure-directing influence of octahedral $\{X_x(H_2O)_{6-x}\}$ ($X = Br^-, Cl^-$; $x = 2, 4, 6$) assemblies that reside inside the hollow cluster shells and determine the arrangement of di- and tetranuclear vanadate units. The approach allows the preparation of a series of high-nuclearity POM cages that are characterized by $\{V_{16}As_8\}$, $\{V_{16}As_{10}\}$, $\{V_{20}As_8\}$, and $\{V_{24}As_8\}$ core structures. In the latter cluster cage, the vanadium centers adopt a truncated octahedral topology. The formation of this Archimedean body is the direct result of the assembly of six square $\{V_4O_8\}$ units that cap the vertices of the encapsulated Platonic $\{Cl_6\}$ octahedron. To the best of our knowledge, this $\{V_{24}As_8\}$ cage is the largest hybrid vanadate cluster reported to date.

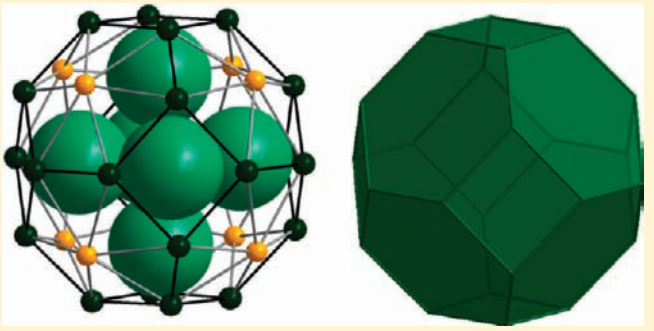

INTRODUCTION

Coordination cages and capsules represent intriguing subclasses of supramolecular compounds whose syntheses and physicochemical characterization have received much attention over the last decades.[1] The topology and connectivity of the metal centers in such nanoscopic systems may give rise to unusual electronic and magnetic properties, while the nature and size of the resulting inner cavities often provide unique restricted chemical environments that allow the molecules to be exploited as catalysts or supramolecular containers or for molecular recognition purposes.[1d,2] Most successful preparative methodologies for metallosupramolecular cages and related compounds take advantage of preorganized, kinetically stable building blocks that provide ligand-accessible coordination sites to direct the assembly into the desired molecules.[3] Polyoxometalates, the clusters of the early transition metal ions, whose electronic and geometrical characteristics enable them to form highly symmetrical structures, provide an intriguing system that can be exploited for the preparation of complex hollow molecular entities.[4,5] Their assembly in aqueous systems is the result of condensation reactions, and the observed structures often comprise distinctive building units that are linked by a set of predetermined connection modes.[3b,6,7]

Two decades ago, Müller stated that polyoxovanadate chemistry is characterized by $\{OVO_4\}$ square pyramids whose condensations give rise to the formation of different hollow structures depending on the size, shape, and charge of an encapsulating species (template).[8] This concept is not restricted to purely inorganic cluster species.[9] Moreover, it is applicable to hybrid guest–host systems that are stabilized by organophosphonate and -arsonate ligands, such as $[2H_2O\subset V_{12}O_{12}(OH)_2(H_2O)_2(PhAsO_3)_{10}(PhAsO_3H)_4]^{2-}$, $[Cl_4\subset V_{18}O_{25}(H_2O)_2(PhPO_3)_{20}]^{4-}$, $[(H_2O)_2N_3^-\subset V_{14}O_{22}(OH)_4(PhPO_3)_8]^{7-}$, and $[Cl_2\subset(V_{12}O_{20})(H_2O)_{12}(Ph_2CHPO_3)_8]^{2-}$.[10] These structures, which were reported by Müller, Zubieta, and Clearfield, all contain rectangular building units consisting of four or five $\{OVO_4\}$ square pyramids; structural and density functional theory (DFT) analyses have suggested that these and related subunits can provide site-specific receptors for anionic species (e.g., N_3^-, ClO_4^-, and halides) or neutral nucleophiles that may influence or template the condensation into larger capsular entities.[10,11]

In order to restrict the number of degrees of freedom and control the assembly processes, template synthesis has proven to be a very powerful approach within the field of supramolecular chemistry.[12] The aforementioned conceptual ideas are particularly appealing for the construction of new high-symmetry cages wherein the templated assembly of small rectangular subunits might give rise to the controlled formation of highly symmetrical

Received: March 16, 2011
Published: June 17, 2011

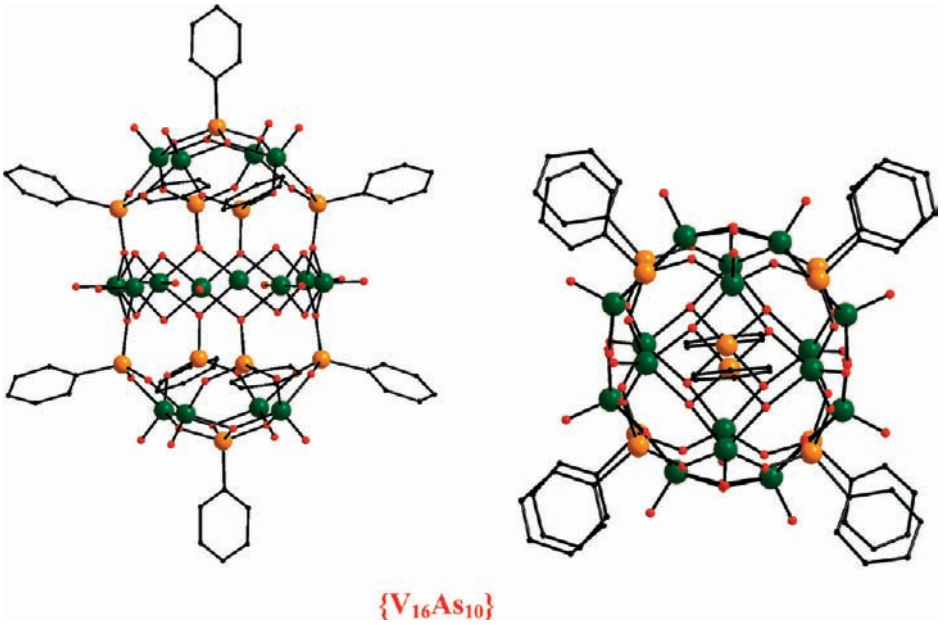

Figure 1. Different perspectives of the structure of $[(V^{IV}O)_{16}(OH)_8(O_4AsC_6H_5)_2(O_3AsC_6H_5)_8]$ (**1**). The encapsulated $\{Br_2(H_2O)_4\}$ guests and the H atoms have been omitted for clarity. Color code: V, green; As, orange; O, red; C, black.

clusters with cubic, truncated octahedral, or rhombicuboctahedral topologies (Archimedean bodies that contain squares).[6d,13]

We are interested in the concept of hybrid organic−inorganic materials, which allows us to combine the advantageous properties of organic and inorganic moieties,[14] and we have previously demonstrated that rigid bifunctional ligands can be used to link preorganized rectangular subunits intramolecularly to generate hybrid organic−inorganic capsules.[15] Herein we report a modular synthetic approach that takes advantage of the described supramolecular templating effect, allowing us to control the assembly of tetranuclear and dinuclear secondary building units to produce a series of high-nuclearity hybrid cluster cages, $[(V^{IV}O)_{16}(OH)_8(O_4AsC_6H_5)_2(O_3AsC_6H_5)_8]$ (isomers **1** and **2**), $[(V^{V}O)_{16}O_{16}(O_3AsC_6H_5)_8]$ (**3**), $[(V^{V}O)_{16}(V^{IV}O)_4O_{16}(OH)_4(O_3AsC_6H_5)_8]^{4+}$ (**4**), and $[(V^{V}O)_{16}(V^{IV}O)_8O_{24}(O_3AsC_6H_5)_8]$ (**5**). The topologies of these hollow structures are determined by the symmetries and compositions of the parent encapsulated aggregates and culminate in a truncated octahedral Archimedean $\{V_{24}\}$ body that encapsulates an octahedral Platonic $\{Cl_6\}$ template.

RESULTS AND DISCUSSION

Synthesis and Structures of $\{V_{16}As_{10}\}$ Isomers in $[\{Br_2(H_2O)_4\}\subset\mathbf{1}]^{2-}$ and $[\{Cl_2(H_2O)_4\}\subset\mathbf{2}]^{2-}$. Modifications of established synthetic protocols[10d] and oxidation of VBr_3 in MeCN in the presence of phenylarsonic acid and triethylamine led to the formation of $[\{Br_2(H_2O)_4\}\subset\mathbf{1}]^{2-}$. X-ray crystallography revealed that the polyoxometalate cage **1** contains 16 square-pyramidally coordinated vanadium atoms and 10 fully deprotonated phenylarsonic acid ligands. As shown in Figure 1, the cage structure of **1** can be described as the symmetric linkage of two convex $\{V^{IV}_4O_5(O_3AsC_6H_5)\}$ moieties to a central $\{(V^{IV}O)_8(\mu_2\text{-}OH)_8\}$ ring unit by eight arsonate functionalities. In the $\{V^{IV}_4O_5(O_3AsC_6H_5)\}$ capping units, a central arsonate ligand links four V^{IV} centers into a square arrangement. This motif is further stabilized by four arsonate ligands, each linking two V atoms in an O,O′-syn,syn bridging mode and binding to the edges of the square. The third O donor of each of the four arsonate functionalities links the capping motif with the central octanuclear ring, providing μ_2-O ligands. Within the ring moiety of **1**, the V centers are alternatively bridged by two μ_2-OH and two μ_2-O arsonate donors that originate from the two $\{V^{IV}_4O_5(O_3AsC_6H_5)\}$ capping units, resulting in a regular $\{-V(\mu_2\text{-}OH)_2-V(\mu_2\text{-}O_{arsonate})_2-\}$ bridging pattern.

We notice that there are two bromide anions and four water molecules encapsulated inside the cavity of the $\{V_{16}As_{10}\}$ cluster cage. These guest molecules are arranged into a symmetrical $\{Br_2(H_2O)_4\}$ octahedron in which the two Br^- ions are situated in the apical positions [Br···H_2O distances: 3.130(1)−3.359(1) Å; Br···Br distance: 5.280(2) Å]. Within the cage, these bromide anions are located at the focal points of the $\{V^{IV}_4O_5(O_3AsC_6H_5)\}$ units and reside 3.466(2)−3.508(3) Å from the vanadium atoms. The four water molecules are located within the plane of the $\{(V^{IV}O)_8(\mu_2\text{-}OH)_8\}$ ring. Each water molecule is situated close to two adjacent vanadium atoms [V···H_2O distances: 2.217(1)−2.603(1) Å], dividing the octanuclear ring into four $\{V_2O_4\}$ subunits. Cage **1** can be regarded as a larger homologue of a series of reported hybrid polyoxovanadates in which tetra- or pentanuclear capping units are linked through two $\{O_4V^{IV}(OH)_2V^{IV}O_4\}$ units.[10,15] Our structural investigation strongly suggested that the nuclearity, size, and topology of the cluster cores are determined by the nature and geometry of the guest assembly located within the capsular entity. This insight prompted us to vary the templating agent, and interestingly, use of VCl_3 as the starting material instead of VBr_3 afforded coordination cluster **2**, which is a constitutional isomer of **1**. In $[\{Cl_2(H_2O)_4\}\subset\mathbf{2}]^{2-}$, the two convex $\{V^{IV}_4O_5(O_3AsC_6H_5)\}$ capping units are rotated 45° with respect to each other, residing in a staggered arrangement that enforces an alternating $\{-V(\mu_2\text{-}OH)(\mu_2\text{-}O_{arsonate})-V(\mu_2\text{-}O_{arsonate})(\mu_2\text{-}OH)V-\}$ bridging pattern within the connecting central octanuclear ring moiety (Figures 2 and 3). Expectedly, and in agreement with the

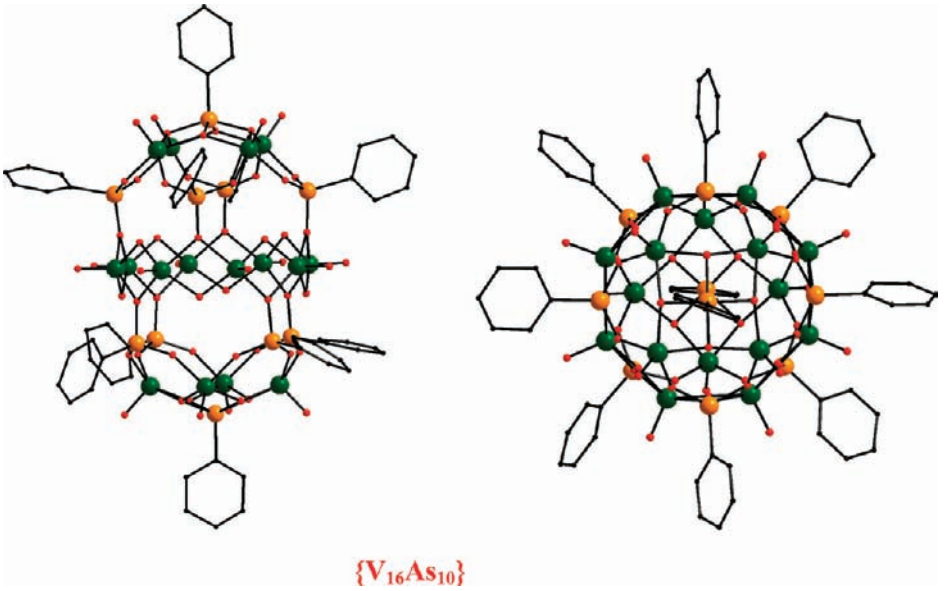

Figure 2. Different perspectives of the structure of $[(V^{IV}O)_{16}(OH)_8(O_4AsC_6H_5)_2(O_3AsC_6H_5)_8]$ (**2**). The encapsulated $\{Cl_2(H_2O)_4\}$ guests and the H atoms have been omitted for clarity. Color code: V, green; As, orange; O, red; C, black.

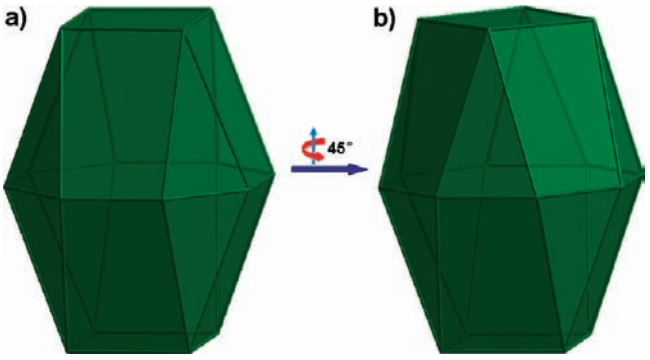

Figure 3. Polyhedral representations highlighting the arrangement of the 16 vanadium atoms in (a) **1** and (b) **2**.

proposed templating effect, a $\{Cl_2(H_2O)_4\}$ octahedron is encapsulated inside the cavity of **2** [Cl···H_2O distances: 3.032(3)−3.177(4) Å; Cl···Cl distance: 5.306(4) Å]. The positions of the Cl atoms and the H_2O molecules are almost identical to those of the corresponding template assembly in **1**. The distances between the chloride anions and the V atoms in the capping motifs are in the range 3.478(4)−3.510(4) Å and almost equal to the V···Br separations in **1**. However, the significantly different ionic radii of Cl^- and Br^- ions and the variation between the V···Cl and V···Br interaction energies[11a] impose the observed structural changes and result in the formation of two different isomers.

Synthesis and Structure of the $\{V_{16}As_8\}$ Cage in $[\{Cl_4(H_2O)_2\}\subset\mathbf{3}]^{2-}$. The structures of **1** and **2** strongly insinuate that the square arrangement of the V atoms is templated by the halide ions while the structure of the ring motif is stabilized by the presence of the water molecules. This conclusion provoked us to explore possibilities to generalize this supramolecular effect and utilize it for the construction of larger and even more symmetric cage structures. From the literature it is known that the condensation reactions and resulting polyoxovanadate types are influenced by the V^V/V^{IV} ratio,[6a,15] and it has been shown that inorganic nitrates provide excellent oxidizing agents for V(III) systems.[16] This redox system is well-established and has been widely used in the field of environmental chemistry for quantitative detection of NO_3^- ions.[17] At elevated temperatures, this process exclusively produces gaseous nitrous oxides that do not interfere with the assembly process as anionic templates. We selected $Dy(NO_3)_3\cdot xH_2O$ ($x \approx 6$) as an oxidant in modified syntheses, also anticipating that the additional metal ions would give rise to new mixed-metal POM structures. This synthetic approach resulted in the formation of the cluster cage $[\{Cl_4(H_2O)_2\}\subset\mathbf{3}]^{2-}$.

As shown in Figure 4, **3** consists of four $\{V_4O_8\}$ units that are connected to each other by eight arsonate ligands, producing a toroidal structure. All the V^V atoms in the $\{V_{16}As_8\}$ cage of **3** form square-pyramidal coordination polyhedra involving terminal oxo ligands, two bridging μ_2-O^{2-} oxo ligands, and two arsonate O donors. Each $\{VO_5\}$ pyramid shares two vertices with two adjacent pyramids, resulting in the formation of a $\{V_4O_8\}$ moiety in which the transition-metal ions adopt a rectangular arrangement. It is apparent that this subunit is structurally closely related to the rectangular $\{V^{IV}{}_4O_5(O_3AsC_6H_5)\}$ capping motifs in **1** and **2**; however, a central arsonate moiety is not present, and the V atoms reside in the higher oxidation state +V, in agreement with the applied experimental conditions. As in **1** and **2**, four arsonate ligands stabilize this tetranuclear motif. Each organic ligand binds via its $\{AsO_3\}$ functionality to the edges of two adjacent square units, linking two V atoms in an O,O′-syn,syn coordination mode. The overall coordination mode of the organic ligands can be described as μ_4-η^1,η^1,η^2. Two μ_2-O arsonate donors deriving from two organic ligands doubly bridge two V atoms, facilitating the connectivity of the $\{V_4O_8\}$ units. As anticipated from the topology of **3**, four Cl^- ions are associated with the four tetranuclear $\{V_4O_8\}$ building units encapsulated inside the $[(V^VO)_{16}O_{16}(O_3AsC_6H_5)_8]$ torus. The four Cl^- anions are situated below the centers of the $\{V_4O_8\}$ units and adopt a square arrangement with closest Cl···Cl distances of

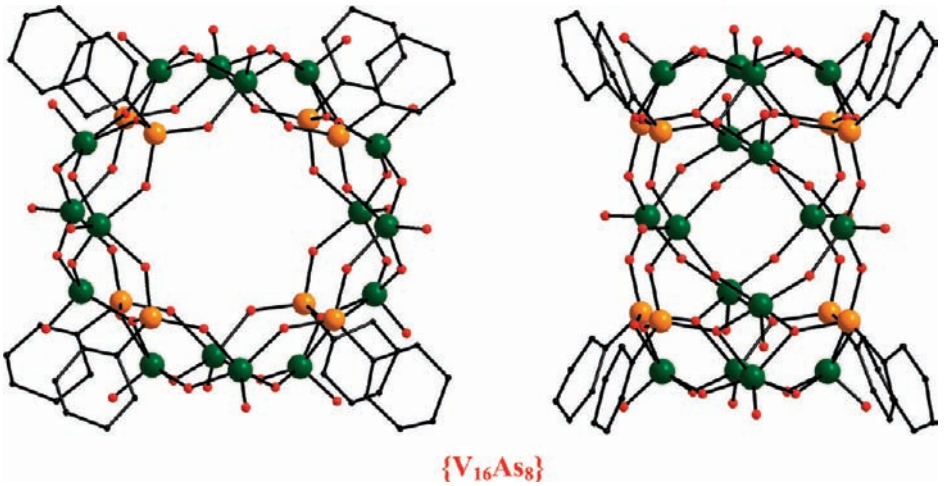

Figure 4. Different perspectives of the toroidal cluster $[(V^{V}O)_{16}O_{16}(O_3AsC_6H_5)_8]$ (**3**). The encapsulated $\{Cl_4(H_2O)_2\}$ guests and the H atoms have been omitted for clarity. Color code: V, green; As, orange; O, red; C, black.

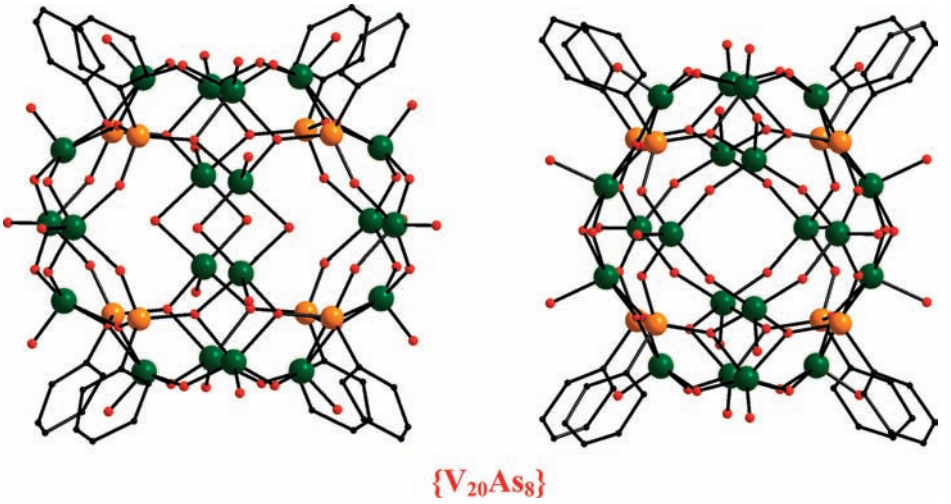

Figure 5. Different perspectives of $[(V^{V}O)_{16}(V^{IV}O)_4O_{16}(OH)_4(O_3AsC_6H_5)_8]^{4+}$ (**4**), which is formally obtained by attaching two linear $\{V_2O_4\}$ building units to the toroidal structure of **3**. The encapsulated $\{Cl_4(H_2O)_2\}$ guests and the H atoms have been omitted for clarity. Color code: V, green; As, orange; O, red; C, black.

3.970(5) Å. Their positions are further characterized by V···Cl distances in the range 2.816(3)−3.021(4) Å. Moreover, two water molecules are encapsulated inside the cavity, and as in **1** and **2**, the guest assembly assumes an octahedral arrangement [Cl···H_2O distance: 3.412(4) Å; H_2O···H_2O distance: 3.881(8) Å]. In agreement with the previously described structures, it appears that the structure and composition of this encapsulated assembly correlates with the nuclearity and topology of the host cluster **3**. In this case, the encapsulated H_2O molecules simply act as guests, but on the basis of the structural studies of **1** and **2**, one would expect them to have the potential to direct the attachment of dinuclear V units in their proximity. Indeed, when we influenced the V^{IV}/V^{V} ratio and decreased the relative amounts of nitrate oxidants during the synthesis, the expected cluster $[\{Cl_4(H_2O)_2\}\subset\mathbf{4}]$ formed.

Structure of the $\{V_{20}As_8\}$ Cage in $[\{Cl_4(H_2O)_2\}\subset 4]$. The $\{V_{20}As_8\}$ core structure of **4** can be visualized as the toroidal structure of **3** decorated with two $\{(V^{IV}O)_2(\mu_2\text{-}OH)_2\}$ units in which the $\{VO_5\}$ square pyramids share common edges (Figures 5 and 6). This decoration is facilitated by the expansion of the coordination mode of the arsonate ligands from

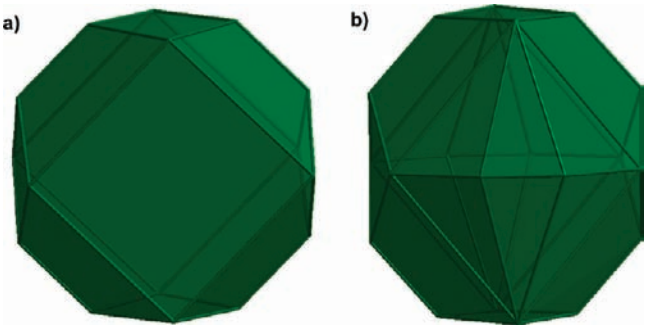

Figure 6. Polyhedral representations of the arrangement of the 16 and 20 vanadium atoms in (a) **3** and (b) **4**.

μ_4-η^1,η^1,η^2 in **3** to μ_5-η^1,η^2,η^2 in **4**, wherein two of the three arsonate O donors of each organic ligand bridge pairs of V centers. The mixed-valent nature of $[(V^{V}O)_{16}(V^{IV}O)_4O_{16}(OH)_4(O_3AsC_6H_5)_8]^{4+}$ (**4**) resulted from the use of lower nitrate mole fractions and was confirmed by bond valence sum analyses: the V centers in the dinuclear units are in oxidation state +IV, while those in the tetranuclear building units assume the +V oxidation state (see Table S1 in the Supporting Information).[18] The atom positions and geometrical parameters of the encapsulated and structure-influencing $\{Cl_4(H_2O)_2\}$ octahedron are almost identical to those in **3** [Cl···Cl distance: 3.982(3) Å; Cl···H_2O distances: 3.240(1)−3.800(1) Å; H_2O···H_2O distance: 4.260(3) Å], with closest V···Cl distances ranging from 2.805(3) to 3.100(3) Å. The two encapsulated H_2O molecules are engaged in interactions with the V centers in the $\{(V^{IV}O)_2(\mu_2\text{-}OH)_2\}$ units. V···O_{water} distances of 2.359(2) Å compare very well to those in **1** and **2**.

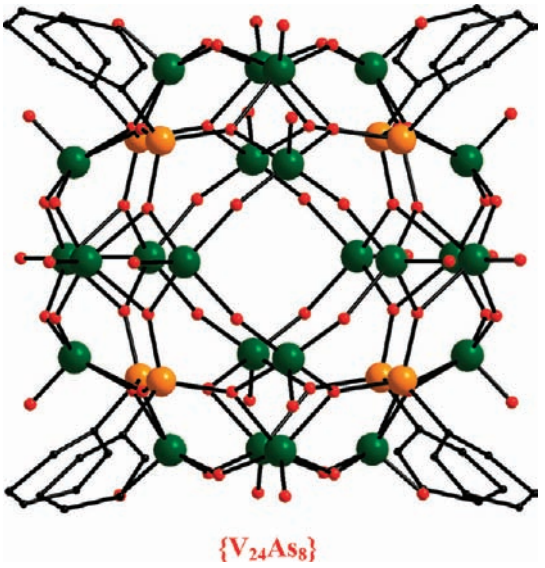

Figure 7. Structure of $[(V^{V}O)_{16}(V^{IV}O)_8O_{24}(O_3AsC_6H_5)_8]$ (**5**), which is formally obtained by attaching two square $\{V_4O_8\}$ building units to the toroidal structure of **3**. The encapsulated $\{Cl_6\}$ guests and the H atoms have been omitted for clarity. Color code: V, green; As, orange; O, red; C, black.

All of the cluster cages **1**−**4** incorporate octahedral $\{X_x(H_2O)_{6-x}\}$ assemblies: **1** and **2** result from the structure-directing influence of $\{X_2(H_2O)_4\}$ (X = Cl^-, Br^-) aggregates, while **3** and **4** are stabilized by $\{Cl_4(H_2O)_2\}$ assemblies. One could plausibly expect that the two encapsulated H_2O molecules in **3** and **4** could also be replaced by Cl^- ions, resulting in a cage structure in which the centers of the $\{V_4O_8\}$ units are symmetrically organized along the vertices of a $\{Cl_6\}$ aggregate. Interestingly, this supramolecular concept rationalizes the formation, composition, and topology of $[\{Cl_6\}\subset\mathbf{5}]$, which was obtained when we further decreased the amount of the nitrate oxidant.

Structure of the $\{V_{24}As_8\}$ Cage in $[\{Cl_6\}\subset\mathbf{5}]$. The structure of **5** and its $\{V_{24}As_8\}$ core are shown in Figure 7. This polyoxovanadate cluster encapsulates a $\{Cl_6\}$ octahedron [Cl···Cl distances: 3.913(5)−4.009(9) Å] that organizes six square $\{V_4O_8\}$ building units into a truncated octahedral topology. The closest V···Cl distances are in the range 2.941(8)−3.033(9) Å. In **5**, all three oxygen donors of each arsonate ligand bridge pairs of vanadium atoms, and their overall coordination mode can be described as μ_6-η^2,η^2,η^2. As in **3** and **4**, the eight As atoms in **5** assume the corner positions of an almost ideal $\{As_8\}$ cube whose faces are capped by six $\{V_4O_8\}$ units. However, in contrast to **3** and **4**, not all of the square-pyramidally coordinated V atoms in the square units are in the +V oxidation state. Bond valence sum analyses confirmed the presence of two $\{V^{V}{}_4O_8\}$ and four $\{V^{IV}{}_2V^{V}{}_2O_8\}$ units. To the best of our knowledge, the cluster cage of $[(V^{V}O)_{16}(V^{IV}O)_8O_{24}(O_3AsC_6H_5)_8]$ (**5**) represents the

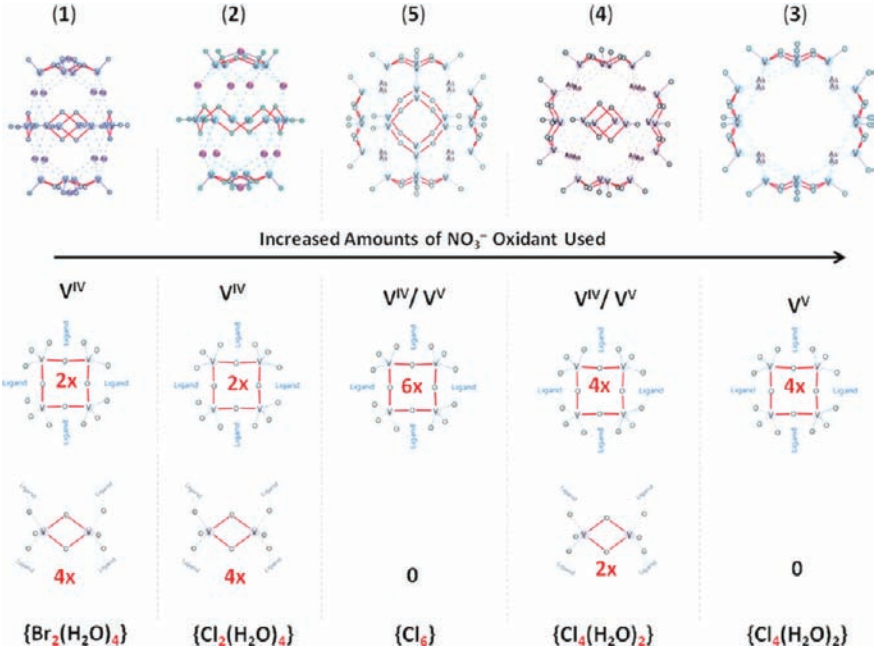

Figure 8. Rationalization of the formation of the cage structures of **1**−**5**. The scheme highlights the encapsulated templates and the appropriate numbers of tetra- and dinuclear building units that are involved in the self-assembly processes for the respective cluster cages. The observed V oxidation states are dependent on the amount of NO_3^- oxidant added during the synthesis of the coordination clusters.

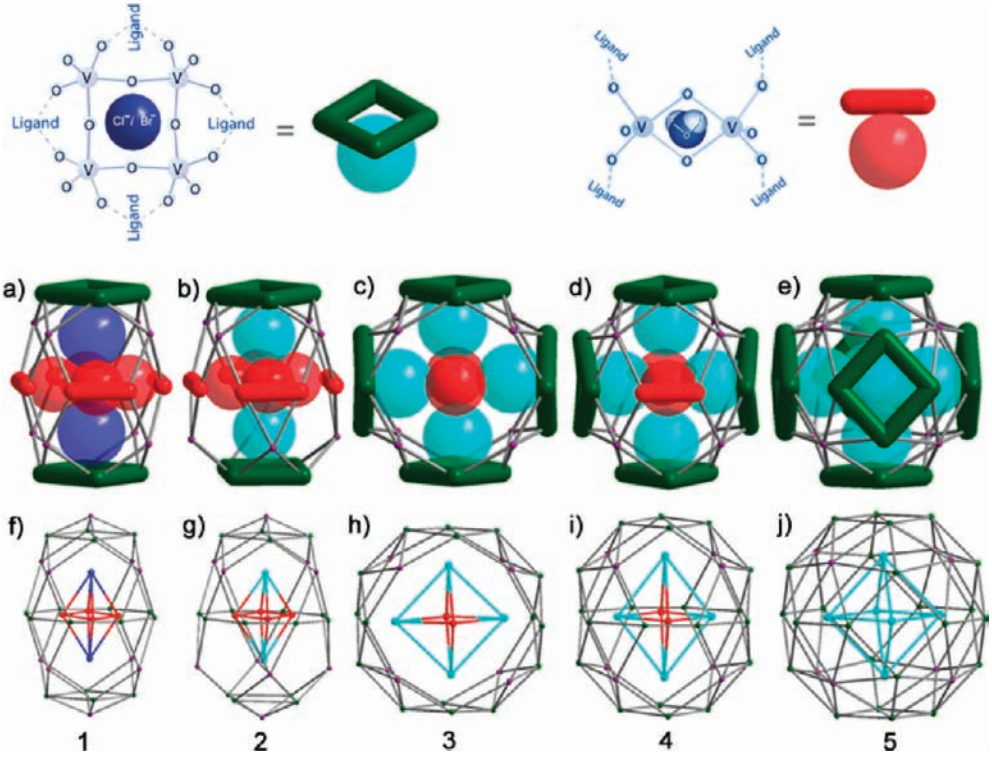

Figure 9. Simplified core structures and their encapsulated templates. (a–e) Schematic representations of the assemblies of the $\{V_4O_8\}$ and $\{V_2O_4\}$ building units to produce **1**–**5** under the influence of the octahedral $\{Br_2(H_2O)_4\}$ and $\{Cl_x(H_2O)_{6-x}\}$ (x = 2, 4, 6) templates. (f–j) Topological representations of **1**–**5** with V and As atoms as connecting nodes. Pictographic representations of the tetra- and dinuclear building units and their corresponding halide and H_2O templates are shown at the top. Color code: V, green; As, violet; O, red; Br, blue; Cl, turquoise.

largest hybrid organic–inorganic polyoxovanadate cluster reported to date.

Successive Cluster Buildup of 1–5. Our applied oxidative synthetic approach allows us to control the V^V/V^{IV} ratios and thereby influence the template and cage formation (Figure 8). The construction of **1**–**5** follows an assembly principle that is characteristic for polyoxovanadates and underlines the fact that the shape and size of $\{OVO_4\}$ square-pyramid-based cluster shells are determined by the encapsulated electrophilic guest species (templates).[8] In our regime, we observed that a series of octahedral $\{X_x(H_2O)_{6-x}\}$ ($X = Br^-$, Cl^-; x = 2, 4, 6) templates influenced the formation of clusters **1**–**5**. The halide ions and H_2O molecules are associated with the formation and assembly of tetranuclear $\{V_4\}$ and dinuclear $\{V_2\}$ secondary building units, respectively. $\{Br_2(H_2O)_4\}$ and $\{Cl_2(H_2O)_4\}$ aggregates support the assembly of two $\{V_4\}$ units and four $\{V_2\}$ units, affording the two constitutional $\{V_{16}As_{10}\}$ isomers **1** and **2** ($V_{16} = 2 \times V_4 + 4 \times V_2$). When two H_2O molecules are formally replaced by two Cl^- ions, a new $\{Cl_4(H_2O)_2\}$ template promotes the formation of $\{V_{16}As_8\}$ cage **3**, in which four $\{V_4\}$ units cap the four Cl^- ions ($V_{16} = 4 \times V_4 + 0 \times V_2$). It is interesting to note that **3** forms reproducibly but in quite low yields, while the next homologue, **4**, which encapsulates an identical $\{Cl_4(H_2O)_2\}$ aggregate, readily forms in higher quantities. This observation can be attributed to the influence of the encapsulated water molecules, which promote decoration with dinuclear vanadium subunits to give the $\{V_{20}As_8\}$ cluster core of **4** ($V_{20} = 4 \times V_4 + 2 \times V_2$). In agreement with the encapsulated octahedral $\{Cl_6\}$ template, **5** consists of six $\{V_4\}$ units that are organized to give a truncated octahedral Archimedean body. Figure 8 rationalizes the formation of the cage structures and further shows that the quantity of NO_3^- oxidants used correlates with the observed oxidation states. We applied electrospray ionization mass spectrometry (ESI-MS) and powder X-ray diffraction (PXRD) experiments to characterize these compounds further (see Figures S12–S18 in the Supporting Information).[19]

Guest–Host Interactions in 1–5. The observed structures and formation processes are in line with those for previously reported polyoxovanadate structures, which reveal strong affinities between tetranuclear $\{V_4O_8\}$ subunits and halides or other electron-rich species. Our observations further agree with DFT calculations that have investigated guest–host interactions of related tetranuclear subunits with bowl or "convex calix" topology.[11a] Calculations of the molecular electrostatic potentials (MEPs) suggest that our tetranuclear subunits provide electrophilic inner environments and nucleophilic outer ones. The observed guest–host interactions most likely originate from the high polarizability of the tetranuclear hosts, which induce significant polarization of the guest anions and result in stabilizing dipole–dipole interactions whereby electron density is transferred from the halide lone pairs to the σ^* orbitals of terminal V–O bonds that point radially toward the outside of the cluster. The observed guest–host energies are expected to be comparable to those of alkali ion/crown ether interactions and are higher for Cl^- than for Br^-.[11a]

Topological analysis of the cage structures in 1–5. We applied topological analyses to rationalize the structures and examine their relationships (Figure 9). The successive buildup of clusters **1**–**5** is associated with a concomitant increase in the As connectivities. The As centers in **1**, **2**, and **3** provide

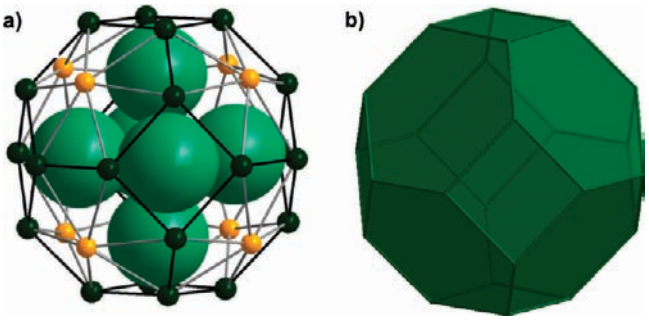

Figure 10. (a) $\{V_{24}As_8\}$ cluster topology with the $\{Cl_6\}$ template highlighted using the space-filling representation. (b) Truncated octahedral arrangement of the 24 vanadium atoms in **5** to give an Archimedean body.

four-connecting nodes; in **4**, the As atoms represent five-connecting nodes, while in **5**, all of the As atoms impart six-connecting vertices. The topologies and symmetries of the cluster compounds obtained by treating the As and V atoms as nodes and the bridging O atoms as linkers are highlighted in Figure 9.

If one omits the As atoms and considers only the V nodes, it is apparent that the 24 vanadium atoms in **5** extend through bridging O atoms to form an enclosed V_{24} cage. Its ideal truncated octahedral topology and O_h symmetry are the direct result of the assembly of six square $\{V_4O_8\}$ units that cap the vertices of the encapsulated $\{Cl_6\}$ octahedron. The observed tiling motif, whereby a square and two hexagons connect at each of the 24 V nodes [vertex symbol (4,6,6)] is also characteristic for β-cages in zeolites, such as in sodalite/aquamarine structures (Figure 10).

Platonic $\{Cl_6\}$ Template and Archimedean $\{V_{24}\}$ Host. Our research results highlight the geometrical relationship between Platonic templates and closed-shell Archimedean solids. A Platonic solid is a convex polyhedron whose faces, edges, vertices, and angles are congruent, with the same number of faces meeting at each vertex. Archimedean solids are defined as semiregular convex polyhedra built of two or more types of regular polygons meeting at identical vertices.[20] Through variation of the reaction conditions, we successively increased the symmetry of the encapsulated template to obtain an ideal $\{Cl_6\}$ octahedron, which represents a Platonic polyhedron. The truncated octahedral $\{V_{24}\}$ cluster core of **5** is characterized by 14 faces, 36 edges, and 24 vertices and can be classified as one of the 13 Archimedean solids (Figure 10). Mathematically a truncated octahedron is constructed from a regular octahedron by the removal of six square pyramids, one from each vertex point. Our investigated supramolecular approach is based on the ability to cap each Cl vertex of the octahedral template by square tetranuclear vanadium units. This synthetic methodology adequately matches the mathematical construction of this Archimedean solid. It is important to note that cluster **5** can be classified as a Keplerate, that is, a cage compound characterized by endohedral, encapsulating arrangements of both Platonic and Archimedean bodies.[21]

CONCLUSION

In summary, we have described a successive buildup of highly symmetrical nanoscopic coordination cages. Our synthetic approach takes advantage of a supramolecular templating effect involving octahedral $\{halide/H_2O\}$ assemblies that form during the formation of the cage and reside in the cluster cavity. The halide ions are associated with the formation and assembly of tetranuclear $\{V_4\}$ secondary building units, while the encapsulated H_2O molecules relate to the stabilization of dinuclear $\{V_2\}$ units. In our regime, the V^V/V^{IV} molar ratio provides us with a tool to influence the involved condensation reactions and control the template and cage formation. Octahedral $\{X_2(H_2O)_4\}$ ($X = Cl^-$, Br^-) aggregates stabilize the two constitutional-$\{V_{16}As_{10}\}$ isomers **1** and **2**, whose conformations are influenced by the nature of the halide involved. $\{Cl_4(H_2O)_2\}$ promotes the formation of the $\{V_{16}As_8\}$ and $\{V_{20}As_8\}$ cluster cores in **3** and **4**, while the Platonic $\{Cl_6\}$ template leads to the $\{V_{24}As_8\}$ core structure in **5**. The latter is the largest hybrid vanadate cluster reported to date, and its formation replicates and agrees with the mathematical relationship between an Archimedean truncated octahedron and an encapsulated Platonic octahedron.

Our investigations have provided a synthetic protocol for controlling the geometrical arrangement of preorganized polynuclear vanadium tectones to produce highly symmetrical coordination cages. It is well-known that several other oxo clusters are stabilized by group-17 ions, and it appears plausible that the outlined synthetic approach can be further generalized and applied to other transition metals. Preliminary investigations that further exploit this supramolecular effect to produce manganese coordination clusters with Archimedean topologies will be reported elsewhere.

EXPERIMENTAL SECTION

Materials and Instrumentation. Commercially available reagents were bought from Sigma-Aldrich or ABCR and used as received without further purification. Fourier transform IR (FTIR) spectroscopic data were collected on a PerkinElmer Spectrum 100 FTIR spectrometer. Elemental analyses (CHN) were obtained from the Microanalysis Lab of the School of Chemistry and Chemical Biology, University College Dublin. PXRD was performed using a Siemens D500 diffractometer with Cu $K\alpha_1$ radiation (λ = 1.54056 Å). ESI-MS data were collected using a time-of-flight MS instrument (LCT Premier, Waters Corp).

Synthesis of $(HNEt_3)_2[\{Br_2(H_2O)_4\}\subset$1$]\cdot 6CH_3CN$. A mixture of VBr_3 (0.290 g, 1.0 mmol), phenylarsonic acid (0.103 g, 0.5 mmol), NEt_3 (0.08 mL), and CH_3CN (25 mL) was stirred and heated to 80 °C for 30 min. The resultant solution was allowed to cool to room temperature, stirred for another hour, and filtered. The filtrate was kept at room temperature, and blue crystals of $(HNEt_3)_2[\{Br_2(H_2O)_4\}\subset$**1**$]\cdot 6CH_3CN$ were obtained within 1 week. Yield: 62% (based on V). CHN anal. calcd (found) for a dried sample with the expected formula $Br_2V_{16}O_{60}C_{72}H_{98}As_{10}N_2$ (corresponding to the crystallographically determined formula after loss of six CH_3CN): C, 23.53 (23.04); H, 2.69 (2.21); N, 0.76 (0.67). IR ν (cm^{-1}): 3355.92 (m), 1440.91 (m), 1091.99 (m), 1003.89 (s), 861.89 (vs), 795.84 (vs), 742.39 (s), 688.62 (vs).

Synthesis of $(HNEt_3)_2[\{Cl_2(H_2O)_4\}\subset$2$]\cdot 2H_2O$. The synthetic procedure was the same as for $(HNEt_3)_2[\{Br_2(H_2O)_4\}\subset$**1**$]\cdot 6CH_3CN$ except that VCl_3 (0.155 g, 1.0 mmol) was used instead of VBr_3. Blue crystals of $(HNEt_3)_2[\{Cl_2(H_2O)_4\}\subset$**2**$]\cdot 2H_2O$ were obtained within 1 week. Yield: 65% (based on V). CHN anal. calcd (found) for $Cl_2V_{16}O_{62}C_{72}H_{102}As_{10}N_2$: C, 23.87 (24.45); H, 2.84 (2.46); N, 0.77 (0.82). IR ν (cm^{-1}): 3367.03 (m), 2921.57 (m), 1440.76 (m), 1092.11 (m), 1002.66 (s), 860.01 (vs), 804.74 (vs), 743.11 (s), 689.06 (s).

Synthesis of $H_5[\{Cl_4(H_2O)_2\}\subset$3$]Cl\cdot 4H_2O\cdot 3CH_3CN$. The synthetic procedure was the same as for $(HNEt_3)_2[\{Cl_2(H_2O)_4\}\subset$**2**$]\cdot 2H_2O$, except that $Dy(NO_3)_3\cdot xH_2O$ (0.149 g) was introduced as a starting material. Green crystals of $H_5[\{Cl_4(H_2O)_2\}\subset$**3**$]Cl\cdot 4H_2O\cdot 3CH_3CN$ were obtained within 3 weeks. Yield: 12% (based on V). CHN anal. calcd (found) for $Cl_5V_{16}O_{62}C_{54}H_{66}As_8N_3$: C, 19.41 (18.61); H, 1.99 (1.85); N, 1.26 (1.17). IR ν (cm^{-1}): 3337.88 (s), 1632.53 (m),

Table 1. Crystal Data and Structure Refinements for (a) $(HNEt_3)_2[\{Br_2(H_2O)_4\}\subset\mathbf{1}]\cdot 6CH_3CN$, (b) $(HNEt_3)_2[\{Cl_2(H_2O)_4\}\subset\mathbf{2}]\cdot 2H_2O$, (c) $H_5[\{Cl_4(H_2O)_2\}\subset\mathbf{3}]Cl\cdot 4H_2O\cdot 3CH_3CN$, (d) $[\{Cl_4(H_2O)_2\}\subset\mathbf{4}]\cdot 7H_2O\cdot 3CH_3CN$, and (e) $H_{10}[\{Cl_6\}\subset\mathbf{5}]Cl_4\cdot 10H_2O\cdot 2CH_3CN$

	a	b	c	d	e
formula	$V_{16}As_{10}Br_2C_{84}H_{84}N_8O_{60}$	$V_{16}As_{10}Cl_2C_{60}H_{47}O_{62}$	$V_{16}As_8Cl_5C_{48}H_{32}O_{62}$	$V_{20}As_8Cl_4C_{48}H_{40}O_{73}$	$V_{24}As_8Cl_{10}C_{48}H_{32}O_{73}$
M_r	3889.64	3395.12	3192.39	3544.76	3953.16
cryst syst	monoclinic	triclinic	tetragonal	orthorhombic	tetragonal
space group	$P2_1/c$	$P\bar{1}$	$I4/m$	$Immm$	$I4/mmm$
a (Å)	17.151(3)	14.081(3)	22.342(3)	17.300(3)	16.028(2)
b (Å)	17.537(3)	17.115(3)	22.342(3)	16.251(3)	16.028(2)
c (Å)	26.583(8)	29.922(6)	14.023(3)	23.716(10)	27.269(5)
α (deg)	90.00	88.90(3)	90.00	90.00	90.00
β (deg)	126.43(2)	85.19(3)	90.00	90.00	90.00
γ (deg)	90.00	65.84(3)	90.00	90.00	90.00
V (Å^3)	6433(2)	6555(2)	7000(2)	6668(3)	7005.3(18)
Z	2	2	2	2	2
T (K)	150	150	150	150	150
ρ_c (g cm^{-3})	2.008	1.708	1.515	1.766	1.874
μ (mm^{-1})	4.369	3.705	3.055	3.462	3.662
coll. reflns	11398	23249	3225	4531	1763
unique reflns	8482	12735	2496	4033	1451
GOF	1.033	1.022	0.985	1.081	1.033
R_1 $[I > 2\sigma(I)]^a$	0.0928	0.0937	0.0818	0.0731	0.1145
wR_2 $[I > 2\sigma(I)]^b$	0.1911	0.2135	0.2178	0.2495	0.2658

$^a R_1 = \Sigma||F_o| - |F_c||/\Sigma|F_o|$. $^b wR_2 = \{\Sigma[w(F_o^2 - F_c^2)^2]/\Sigma[w(F_o^2)^2]\}^{1/2}$.

1482.41 (w), 1439.81 (m), 1184.91 (w), 1087.09 (m), 968.73 (s), 832.10 (vs), 740.33 (vs), 685.24(s).

Synthesis of $[\{Cl_4(H_2O)_2\}\subset\mathbf{4}]\cdot 7H_2O\cdot 3CH_3CN$. The synthetic procedure was the same as for $(HNEt_3)_2[\{Cl_2(H_2O)_4\}\subset\mathbf{2}]\cdot 2H_2O$, except that $Dy(NO_3)_3\cdot xH_2O$ (0.120 g) was introduced as a starting material. Green crystals of $[\{Cl_4(H_2O)_2\}\subset\mathbf{4}]\cdot 7H_2O\cdot 3CH_3CN$ were obtained within 2 weeks. Yield: 58% (based on V). CHN anal. calcd (found) for $Cl_4V_{20}O_{73}C_{54}H_{71}As_8N_3$: C, 17.58 (18.56); H, 1.94 (2.05); N, 1.14 (1.16). IR ν (cm^{-1}): 3336.19 (s), 1633.49 (m), 1481.94 (w), 1439.78 (m), 1087.73 (m), 979.80 (s), 831.41 (vs), 772.08 (vs).

Synthesis of $H_{10}[\{Cl_6\}\subset\mathbf{5}]Cl_4\cdot 10H_2O\cdot 2CH_3CN$. The synthetic procedure was the same as for $(HNEt_3)_2[\{Cl_2(H_2O)_4\}\subset\mathbf{2}]\cdot 2H_2O$, except that $Dy(NO_3)_3\cdot xH_2O$ (0.111 g) was introduced as a starting material. Green crystals of $H_{10}[\{Cl_6\}\subset\mathbf{5}]Cl_4\cdot 10H_2O\cdot 2CH_3CN$ were obtained within 2 weeks. Yield: 52% (based on V). CHN anal. calcd (found) for $Cl_{10}V_{24}O_{82}C_{52}H_{76}As_8N_2$: C, 14.81 (14.57); H, 1.82 (1.95); N, 0.66 (0.80). IR ν (cm^{-1}): 3327.68 (s), 1634.49 (s), 1482.97 (w), 1439.99 (m), 1185.33 (w), 1087.48 (m), 979.36 (s), 791.07 (vs), 683.56(s).

X-ray Crystallography. Single-crystal X-ray structure determinations of the five compounds (**a**) $(HNEt_3)_2[\{Br_2(H_2O)_4\}\subset\mathbf{1}]\cdot 6CH_3CN$, (**b**) $(HNEt_3)_2[\{Cl_2(H_2O)_4\}\subset\mathbf{2}]\cdot 2H_2O$, (**c**) $H_5[\{Cl_4(H_2O)_2\}\subset\mathbf{3}]Cl\cdot 4H_2O\cdot 3CH_3CN$, (**d**) $[\{Cl_4(H_2O)_2\}\subset\mathbf{4}]\cdot 7H_2O\cdot 3CH_3CN$, and (**e**) $H_{10}[\{Cl_6\}\subset\mathbf{5}]Cl_4\cdot 10H_2O\cdot 2CH_3CN$ were performed at 150 K on a Bruker SMART APEX diffractometer using graphite-monochromatized Mo Kα radiation. Absorption corrections were applied using *SADABS*.[22] Structures were solved by direct methods and refined by full-matrix least-squares on F^2 using *SHELXTL*.[23] For structures **b**−**e**, some solvent molecules were highly disordered and could not be located. The provided formulas were obtained from the combination of crystallographic and elemental analysis.

Contributions to scattering due to disordered solvent molecules were removed using the *SQUEEZE* routine of *PLATON*;[24] structures were then refined again using the data generated. In **e**, the chloride counterion located outside the cluster was highly disordered. This effect resulted in higher U_{eq} values for the adjacent O6, V2, and V3 atom positions and slightly higher quality values for this structure. Crystal data and details of data collection and refinement for **a**−**e** are summarized in Table 1. The crystallographic data have been deposited with the Cambridge Crystallographic Data Centre (CCDC) as entries 798576−798580 and can be obtained free of charge via www.ccdc.cam.ac.uk/data_request/cif.

■ ASSOCIATED CONTENT

Supporting Information. Table S1, Figures S1−S18, and crystallographic data (CIF) for the new structures. This material is available free of charge via the Internet at http://pubs.acs.org.

■ AUTHOR INFORMATION

Corresponding Author
schmittw@tcd.ie

■ ACKNOWLEDGMENT

The authors thank Science Foundation Ireland (SFI) for financial support (06/RFP/CHE173 and 08/IN.1/I2047). Financial support from IRCSET (fellowship for L.Z.) is gratefully acknowledged. We thank Dr. Thomas McCabe, Dr. John Breen, Ms. Camelia Onet, and Dr. Martin Feeney for help with the physicochemical analyses.

■ REFERENCES

(1) (a) Seidel, S. R.; Stang, P. J. *Acc. Chem. Res.* **2002**, *35*, 972. (b) Olenyuk, B.; Whiteford, J. A.; Fechtenkotter, A.; Stang, P. J. *Nature* **1999**, *398*, 796. (c) Sun, Q.-F.; Iwasa, J.; Ogawa, D.; Ishido, Y.; Sato, S.;

Ozeki, T.; Sei, Y.; Yamaguchi, K.; Fujita, M. *Science* **2010**, *328*, 1144. (d) Fiedler, D.; Leung, D. H.; Bergman, R. G.; Raymond, K. N. *Acc. Chem. Res.* **2005**, *38*, 351. (e) Kong, X.-J.; Long, L.-S.; Zheng, Z.; Huang, R.-B.; Zheng, L.-S. *Acc. Chem. Res.* **2010**, *43*, 201.

(2) (a) Kong, X.-J.; Ren, Y.-P.; Long, L.-S.; Zheng, Z.; Huang, R.-B.; Zheng, L.-S. *J. Am. Chem. Soc.* **2007**, *129*, 7016. (b) Pluth, M. D.; Bergman, R. G.; Raymond, K. N. *Acc. Chem. Res.* **2009**, *42*, 1650. (c) Mal, P.; Breiner, B.; Rissanen, K.; Nitschke, J. R. *Science* **2009**, *324*, 1697. (d) Inokuma, Y.; Arai, T.; Fujita, M. *Nat. Chem.* **2010**, *2*, 780.

(3) (a) Tranchemontagne, D. J.; Ni, Z.; O'Keeffe, M.; Yaghi, O. M. *Angew. Chem., Int. Ed.* **2008**, *47*, 5136. (b) Long, D.-L.; Burkholder, E.; Cronin, L. *Chem. Soc. Rev.* **2007**, *36*, 105.

(4) (a) Topical issue on polyoxometalates: Hill, C. L. *Chem. Rev.* **1998**, *98*, 1 and subsequent articles. (b) *Polyoxometalates: From Platonic Solids to Anti-Retroviral Activity*; Pope, M. T., Müller, A., Eds.; Kluwer: Dordrecht, The Netherlands, 1994. (c) *Polyoxometalate Chemistry: From Topology via Self-Assembly to Applications*; Pope, M. T., Müller, A., Eds.; Kluwer: Dordrecht, The Netherlands, 2001.

(5) (a) Long, D.-L.; Tsunashima, R.; Cronin, L. *Angew. Chem., Int. Ed.* **2010**, *49*, 1736. (b) Botar, B.; Kögerler, P.; Hill, C. L. *J. Am. Chem. Soc.* **2006**, *128*, 5336. (c) Müller, A.; Krickemeyer, E.; Bögge, H.; Schmidtmann, M.; Peters, F. *Angew. Chem., Int. Ed.* **1998**, *37*, 3360. (d) Yan, J.; Gao, J.; Long, D.-L.; Miras, H. N.; Cronin, L. *J. Am. Chem. Soc.* **2010**, *132*, 11410. (e) Kortz, U.; Müller, A.; van Slageren, J.; Schnack, J.; Dalal, N. S.; Dressel, M. *Coord. Chem. Rev.* **2009**, *253*, 2315.

(6) (a) Dolbecq, A.; Dumas, E.; Mayer, C. R.; Mialane, P. *Chem. Rev.* **2010**, *110*, 6009 and references therein. (b) Kang, J.; Xu, B. B.; Peng, Z. H.; Zhu, X. D.; Wei, Y. G.; Powell, D. R. *Angew. Chem., Int. Ed.* **2005**, *44*, 6902. (c) Xiao, F. P.; Hao, J.; Zhang, J.; Lv, C. L.; Yin, P. C.; Wang, L. S.; Wei, Y. G. *J. Am. Chem. Soc.* **2010**, *132*, 5956. (d) Zheng, S. T.; Zhang, J.; Li, X. X.; Fang, W. H.; Yang, G. Y. *J. Am. Chem. Soc.* **2010**, *132*, 15102. (e) Chen, Q.; Goshorn, D. P.; Scholes, C. P.; Tan, X. L.; Zubieta, J. *J. Am. Chem. Soc.* **1992**, *114*, 4667.

(7) (a) Schäffer, C.; Merca, A.; Bögge, H.; Todea, A. M.; Kistler, M. L.; Liu, T. B.; Thouvenot, R.; Gouzerh, P.; Müller, A. *Angew. Chem., Int. Ed.* **2009**, *48*, 149. (b) Todea, A. M.; Merca, A.; Bögge, H.; Glaser, T.; Engelhardt, L.; Prozorov, R.; Lubanc, M.; Müller, A. *Chem. Commun.* **2009**, 3351. (c) Hagrman, P. J.; Hagrman, D.; Zubieta, J. *Angew. Chem., Int. Ed.* **1999**, *38*, 2639.

(8) (a) Müller, A. *Nature* **1991**, *352*, 115. (b) Pope, M. T. *Nature* **1992**, *355*, 27. (c) Müller, A.; Reuter, H.; Dillinger, S. *Angew. Chem., Int. Ed. Engl.* **1995**, *34*, 2328.

(9) (a) Müller, A.; Rohlfing, R.; Döring, J.; Penk, M. *Angew. Chem., Int. Ed. Engl.* **1991**, *30*, 588. (b) Müller, A.; Penk, M.; Rohlfing, R.; Krickemeyer, E.; Döring, J. *Angew. Chem., Int. Ed. Engl.* **1990**, *29*, 926. (c) Chen, L.; Jiang, F. L.; Lin, Z. Z.; Zhou, Y. F.; Yue, C. Y.; Hong, M. C. *J. Am. Chem. Soc.* **2005**, *127*, 8588.

(10) (a) Khan, M. I.; Zubieta, J. *Angew. Chem., Int. Ed. Engl.* **1994**, *33*, 760. (b) Salta, J.; Chen, Q.; Chang, Y.-D.; Zubieta, J. *Angew. Chem., Int. Ed. Engl.* **1994**, *33*, 757. (c) Müller, A.; Hovemeier, K.; Krickemeyer, E.; Bögge, H. *Angew. Chem., Int. Ed. Engl.* **1995**, *34*, 779. (d) Konar, S.; Clearfield, A. *Inorg. Chem.* **2008**, *47*, 3492. (e) Khanra, S.; Kloth, M.; Mansaray, H.; Muryn, C. A.; Tuna, F.; Sañudo, E. C.; Helliwell, M.; McInnes, E. J. L.; Winpenny, R. E. P. *Angew. Chem., Int. Ed.* **2007**, *46*, 5568.

(11) (a) Song, P.; Guan, W.; Yan, L.; Liu, C.; Yao, C.; Su, Z. *Dalton Trans.* **2010**, *39*, 3706. (b) Rohmer, M.-M.; Devémy, J.; Wiest, R.; Bénard, M. *J. Am. Chem. Soc.* **1996**, *118*, 13007. (c) Rohmer, M.-M.; Bénard, M.; Blaudeau, J.-P; Maestre, J.-M.; Poblet, J.-M. *Coord. Chem. Rev.* **1998**, *178*−*180*, 1019.

(12) (a) Miras, H. N.; Cooper, G. J. T.; Long, D.-L.; Bögge, H.; Müller, A.; Streb, C.; Cronin, L. *Science* **2010**, *327*, 72. (b) Bontchev, R. P.; Do, J.; Jacobson, A. J. *Angew. Chem., Int. Ed.* **1999**, *38*, 1937. (c) Müller, A.; Krickemeyer, E.; Penk, M.; Rohlfing, R.; Armatage, A.; Bögge, H. *Angew. Chem., Int. Ed. Engl.* **1991**, *30*, 1674. (d) Müller, A.; Hovemeier, K.; Rohlfing, R. *Angew. Chem., Int. Ed. Engl.* **1992**, *31*, 1192.

(13) (a) Mitchell, S. G.; Streb, C.; Miras, H. N.; Boyd, T.; Long, D.-L.; Cronin, L. *Nat. Chem.* **2010**, *2*, 308. (b) Leininger, S.; Fan, J.; Schmitz, M.; Stang, P. J. *Proc. Natl. Acad. Sci. U.S.A.* **2000**, *97*, 1380.

(14) (a) Schmitt, W.; Hill, J. P.; Malik, S.; Volkert, C.; Ichinose, I.; Anson, C. E.; Powell, A. K. *Angew. Chem., Int. Ed.* **2005**, *44*, 7048. (b) Pelleteret, D.; Clérac, R.; Mathonière, C.; Harté, E.; Schmitt, W.; Kruger, P. E. *Chem. Commun.* **2009**, 221.

(15) Breen, J. M.; Schmitt, W. *Angew. Chem., Int. Ed.* **2008**, *47*, 6904.

(16) Braman, R. S.; Hendrix, S. A. *Anal. Chem.* **1989**, *61*, 2715.

(17) Miranda, K. M.; Espey, M. G.; Wink, D. A. *Nitric Oxide* **2001**, *5*, 62.

(18) Brown, I. D. *J. Appl. Crystallogr.* **1996**, *29*, 479.

(19) (a) Long, D.-L.; Streb, C.; Song, Y.-F.; Mitchell, S.; Cronin, L. *J. Am. Chem. Soc.* **2008**, *130*, 1830. (b) Miras, H. N.; Wilson, E. F.; Cronin, L. *Chem. Commun.* **2009**, 1297. (c) Onet, C. I.; Zhang, L.; Clérac, R.; Denis, B.-J.; Feeney, M.; McCabe, T.; Schmitt, W. *Inorg. Chem.* **2011**, *50*, 604.

(20) (a) Moulton, B.; Lu, J.; Mondal, A.; Zaworotko, M. J. *Chem. Commun.* **2001**, 863. (b) Alvarez, S. *Dalton Trans.* **2005**, 2209.

(21) (a) Müller, A. *Nature* **2007**, *447*, 1035. (b) Müller, A.; Kögerler, P.; Dress, A. W. M. *Coord. Chem. Rev.* **2001**, *222*, 193.

(22) Sheldrick, G. M. *SADABS: Program for Area Detector Adsorption Correction*; University of Göttingen: Göttingen, Germany, 1996.

(23) Sheldrick, G. M. *SHELXL-97: Program for Solution of Crystal Structures*; University of Göttingen: Göttingen, Germany, 1997.

(24) Vandersluis, P.; Spek, A. L. *Acta Crystallogr., Sect. A* **1990**, *46*, 194.